Journal of Cerebral Blood Flow & Metabolism (2013) 33, 583–592

www.jcbfm.com

ORIGINAL ARTICLE

Nanoparticles for targeted delivery of antioxidant enzymes to the brain after cerebral ischemia and reperfusion injury

Xiang Yun[1], Victor D Maximov[1], Jin Yu[2], Hong Zhu[2], Alexey A Vertegel[1] and Mark S Kindy[1,2,3,4]

Stroke is one of the major causes of death and disability in the United States. After cerebral ischemia and reperfusion injury, the generation of reactive oxygen species (ROS) and reactive nitrogen species may contribute to the disease process through alterations in the structure of DNA, RNA, proteins, and lipids. We generated various nanoparticles (liposomes, polybutylcyanoacrylate (PBCA), or poly(lactide-co-glycolide) (PLGA)) that contained active superoxide dismutase (SOD) enzyme (4,000 to 20,000 U/kg) in the mouse model of cerebral ischemia and reperfusion injury to determine the impact of these molecules. In addition, the nanoparticles were untagged or tagged with nonselective antibodies or antibodies directed against the *N*-methyl-D-aspartate (NMDA) receptor 1. The nanoparticles containing SOD protected primary neurons *in vitro* from oxygen-glucose deprivation (OGD) and limited the extent of apoptosis. The nanoparticles showed protection against ischemia and reperfusion injury when applied after injury with a 50% to 60% reduction in infarct volume, reduced inflammatory markers, and improved behavior *in vivo*. The targeted nanoparticles not only showed enhanced protection but also showed localization to the CA regions of the hippocampus. Nanoparticles alone were not effective in reducing infarct volume. These studies show that targeted nanoparticles containing protective factors may be viable candidates for the treatment of stroke.

Journal of Cerebral Blood Flow & Metabolism (2013) **33,** 583–592; doi:10.1038/jcbfm.2012.209; published online 6 February 2013

Keywords: anti-oxidants; antibody; cerebral ischemia; nanoparticles; superoxide dismutase

INTRODUCTION

The long-term outcome of an injury involving central nervous system (CNS) depends on the extent of secondary neuronal damage produced by a series of cellular and molecular events initiated by the primary trauma.[1] Secondary injury is a combination of several factors contributing to cell death, including glutamatergic toxicity, free radical damage, cytokines, and inflammation.[2,3] Secondary oxidative damage caused by elevated levels of ROS, such as superoxide, peroxide, and hydroxyl radicals, is a key neuropathologic process that contributes to ischemia, trauma, and degenerative disorders.[4,5] Central nervous system is particularly susceptible to free radical damage because of the high lipid content.[6] Intravenous steroids (e.g., methylprednisolone sodium succinate) have been approved for clinical use in acute spinal cord injury in many countries and currently are the only available therapeutic option for limiting effects of secondary CNS injury (CNSI).[7] However, safety and efficacy of methylprednisolone sodium succinate therapy is debatable. A recent review of randomized trials concluded that using methylprednisolone sodium succinate did not result in significantly improved outcomes in most cases.[8] Severe side effects were also reported. Thus, the need for development of novel therapeutic strategies for treatment of secondary CNSI is evident.

Numerous studies over the years have shown that ROS have an important role in the pathogenesis of ischemia and reperfusion injury and other neurologic disorders.[9] The reduction in blood flow to the brain result in ischemic injury, while the reoxygenation during reperfusion allows for the generation of oxygen radicals that can further injure the tissue.[9–11] Scavenging of the free radicals by superoxide dismutase (SOD), glutathione peroxidase (GSH-Px), and catalase (CAT) protects the brain from the detrimental effects.[12] The overproduction of ROS in the mitochondria after ischemia and reperfusion injury and the failure of the endogenous antioxidants to detoxify these entities results in an accumulation of ROS.[12] This accumulation of ROS results in the activation of various cellular pathways that trigger damage and death.[10–12] Therefore, targeting antioxidant enzymes as a therapeutic approach for treating ischemia and reperfusion injury is logical and reasonable.

Superoxide dismutase is of special interest as a potential therapeutic agent for secondary CNSI because of its high ROS degradation rate.[13] It converts superoxide, the most toxic ROS, to much less reactive peroxide.[14] Overexpression of SOD1 has been shown to attenuate apoptotic cells death.[15] However, exogenous SOD has shown no efficacy in treatment of secondary CNSI.[16] Previous studies have shown that polyethylene glycol modified SOD may be protective after cerebral ischemia but the effects were equivicol.[17–21] One problem associated with the therapeutic use of antioxidants for CNSI is their limited ability to penetrate through blood–brain barrier (BBB).[22] However, during cerebral ischemia and reperfusion injury studies have shown that the BBB has a biphase opening, which might assist in the delivery of drugs to the brain.[23–26]

[1]Department of Bioengineering, Clemson University, Clemson, South Carolina, USA; [2]Department of Neurosciences, Medical University of South Carolina, Charleston, South Carolina, USA; [3]Ralph H. Johnson VA Medical Center, Charleston, South Carolina, USA and [4]CU/MUSC Bioengineering Research Program, Charleston, South Carolina, USA. Correspondence: MS Kindy, Department of Neurosciences, Medical University of South Carolina, Charleston, SC 29425, USA.
E-mail: kindyms@musc.edu
This work was partially supported by grants from the National Institutes of Health (R01 ES016774-01, 5 P20 RR016461, 8P20GM103444-04, and 5P20RR021949-03), VA Merit Award, and a grant from the National Science Foundation (IIP-917987). Dr Kindy is a Research Career Scientist in the VA.
Received 16 October 2012; revised 26 November 2012; accepted 12 December 2012; published online 6 February 2013

Recently, Reddy *et al*[27] showed that SOD incorporated into PLGA nanoparticles (NPs) showed neuroprotective efficacy against the oxidative challenge in a cell culture model. An *in vivo* study performed by the same group found that intracarotid injection of SOD-loaded PLGA NPs significantly improved the outcome of secondary injury in a rat stroke model.[28] Interestingly, improved therapeutic outcome was only observed in the case of intracarotid injection, but not in the case of intrajugular or tail vein injection. This result was found to be in good agreement with NP biodistribution data: 1.5% of the NPs were delivered to the brain in the case of intracarotid administration, while $\sim$0.1% of NPs was delivered to the brain in the case of either intrajugular or tail vein administration. It was also found that injection of unconjugated SOD did not improve the outcomes. These data point out to the importance of targeted delivery to CNS for *in vivo* therapeutic applications and suggest that further development of more robust delivery systems may lead to improved outcomes of secondary neuronal injury.

Ability of several drug delivery agents to penetrate through BBB has been shown previously and may assist in the administration of compounds to treat neurologic disorders.[29] These agents include biodegradable PBCA NPs or liposomes conjugated to a cell-penetrating peptide.[30] While BBB penetration is essential, it can be assisted to some extent by the above-mentioned biphasic opening during cerebral ischemia and reperfusion injury. Further improvement of efficacy can be achieved by better retention of the antioxidant agent at the injury site. With that in mind, we hypothesized that simultaneous conjugation of SOD and a targeting ligand (such as antibody or cell-penetrating peptide) to delivery vectors (such as NPs or liposomes) could lead to a better uptake by CNS. We have recently performed an *in vitro* study that showed preferential uptake of PBCA NPs simultaneously coated by SOD and targeting anti-NMDA (*N*-methyl-D-aspartate) receptor 1 (NR1) antibody (anti-NR1-SOD-PBCA NPs) by primary rat cerebellar neuron cultures.[31] These NPs were found to be highly neuroprotective against challenge by superoxide in the same cell culture model.[31] Here, we evaluated *in vivo* efficacy of several SOD delivery vectors in a mouse cerebral artery occlusion model, with special attention paid to the effect of targeted delivery. Anti-NR1 receptor antibody was used as the targeting ligand. In the case of untargeted conjugates, a nonspecific secondary rabbit anti-bovine antibody was used instead of anti-NR1 antibody in otherwise identical preparation conditions. The SOD-coated PBCA NPs were prepared using an optimized method compared with that reported in our *in vitro* study.[31] Alternatively, PEGylated liposomes with the lipid composition mimicking that of FDA approved liposomal drug, Doxil, were used as the drug carriers.[32] As in the case of PBCA NPs, both therapeutic enzyme and the targeting ligand were simultaneously conjugated to the surface of the liposomal vectors using a PEGylated maleimide-terminated phospholipid as the crosslinker.[33] Finally, we used SOD-loaded PLGA NPs similar to those reported by Reddy *et al*,[27,28] as a reference system for which efficacy has previously been established. In this case, SOD was loaded in the bulk of the NPs using double emulsion method. Untargeted bulk-loaded PLGA NPs served as the benchmark and were used as prepared. To study effect of targeting, we also decorated the surface of these bulk-loaded SOD-PLGA NPs by anti-NR1 antibody using the same crosslinking chemistry as in our *in vitro* study.[31] The goal of this study was to determine whether enhanced delivery of targeted antioxidant NPs to the site of neuronal injury can reduce the degree of secondary damage.

MATERIALS AND METHODS

Reagents

DNase, RNase, Protease-free water (#327390010) was purchased from Acros Organics (Morris Plains, NJ, USA). n-Butylcyanoacrylate was generously gifted by Tong Shen Ent. Co., Ltd. (Kaohsiung City, Taiwan). HEPES buffer (#BDH4518) was purchased from VWR (West Chester, PA, USA). AlexaFluor 594 (#A20004) fluorescent dye was purchased from Invitrogen Life Technologies Corp. (Carlsbad, CA, USA). Cross-linker sulfo-NHS-LC-Diazirine (#26174) and Traut's Reagent (2-Iminothiolane · HCl) (#26101) were purchased from Thermo Scientific (Waltham, MA, USA). Superoxide dismutase from bovine liver (3,000 u/mg, #574594) was obtained from Calbiochem (Gibbstown, NJ, USA). Anti-Glutamate Receptor NMDAR1 (NR1) IgG produced in rabbit (#G8913) and nonspecific rabbit anti-bovine IgG (whole molecule) (#B5645) were purchased from Sigma-Aldrich (St Louis, MO, USA). According to manufacturer's information sheet, anti-NR1 antibody is specific to synthetic peptide corresponding to the C-terminal region of rat NMDAR1 (amino acids 918 to 938). This sequence is identical in mouse NR1, human NR1 (short and long forms), and rat NR1 isoforms NR1b, NR1c, and NR1f. L-a-Phosphatidylcholine, Hydrogenated (Soy) (#840058), cholesterol (#700100), 1,2-Distearoyl-sn-Glycero-3-Phosphoethanolamine-N-[Methoxy(Polyethylene glycol)-2000] (mPEG2000-DSPE, #880120), and 1,2-Distearoyl-sn-Glycero-3-Phosphoethanolamine-N-[Maleimide(Polyethylene glycol)-2000] (MAL-PEG2000-DSPE, #880126) were purchased from Avanti Polar Lipid Inc. (Alabaster, AL, USA).

Poly(D,L-lactide-co-glycolide) (#P2066, lactide to glycolide ratio 65:35, Mw 40,000 to 75,000), rabbit serum Albumin (RSA, #A6414), and SOD assay kit were purchased from Sigma-Aldrich. Dextran 70 (#D1449, Mw 70,000), D(+)-sucrose, and D(+)-trehalose dehydrate was purchased from TCI America (Portland, OR, USA). Chloroform, acetone, and dimethylformamide were purchased from Calbiochem.

Preparation of Particles

Polybutylcyanoacrylate nanoparticles. Polybutylcyanoacrylate nanoparticles were prepared as described previously using acidic polymerization medium containing 1% (w/v) dextran in 0.01 mol/L HCl. 1 mL of n-Butylcyanoacrylate monomer (density 1.44 g/cm^3) was added to 200 mL of dextran solution under constant stirring at 500 r.p.m. with a Teflon-coated stirring bar.[31] After overnight polymerization, the reaction was stopped by adding 1 mL of 0.1 mol/L NaOH, and the nanoparticle suspension was filtered twice through filter paper (VWR Grade 410 with 1 μm particle retention) in Buchner funnel via suction filtration to remove crystallized n-Butylcyanoacrylate. Excess of surfactant was removed by repeated centrifugation (4,500 r.c.f., 1.5 hours; Allegra 64 R centrifuge, Beckman Coulter, Brea, CA, USA). After each centrifugation step, the supernatant was removed and the nanoparticles were resuspended in the same volume of HPLC-grade water. Finally, nanoparticles were transferred into centrifuge tubes, centrifuged at 4,500 r.c.f. for 30 minutes and resuspended in 10 mL HEPES buffer (20 mmol/L, pH 6.5).

Preparation of Liposomes. PEGylated liposomes were prepared as previously described.[32] The lipids used were phosphatidylcholine, cholesterol, mPEG2000-DSPE, and MAL-PEG2000-DSPE with the molar ratio of 55:39:4:2. Shortly, lipid components were mixed in chloroform, and dried through rotatory evaporation, forming a thin lipid layer. Later, mixed lipid film was rehydrated by HEPES buffer prepared using RNAse, DNAse free water, and sonicated using a probe sonicator (Omni Ruptor 4000, Kennesaw, GA, USA) at 200 W output for 5 minutes. Total lipid concentration consisted of 10 mg/mL.

Protein Conjugation

Protein conjugation to nanoparticles. First, 5 mg of SOD was dissolved in 1.5 mL of HEPES buffer (20 mmol/L, pH 6.5), and 2.5 mg of Sulfo-NHS-LC-Diazirine, a UV-sensitive crosslinker, was dissolved in 0.5 mL of water and added to the SOD solution. For antibody activation, 50 μL of either anti-NR1 or control rabbit anti-bovine antibody solutions (0.2 mg/mL) was mixed with 100 μL of aqueous solution containing 0.1 mg of the same crosslinker. Where applicable, fluorescent labeling of proteins by AlexaFluor dye was performed simultaneously with the protein activation by the crosslinker. The mixtures were then kept in the incubator shaker for 60 minutes (280 r.p.m., foil covered, room temperature). After incubation, unreacted Sulfo-NHS-LC-Diazirine and unbound fluorescent dye were removed by centrifugation through a Microsep centrifugation device (10 kDa MWCO—SOD and 30 kDa—antibodies obtained from Pall Co., (Port Washington, NY, USA). Activated proteins were then collected from the centrifugal device and resuspended in 20 mmol/L HEPES buffer to total volume of 100 and 50 μL for SOD and antibodies, respectively. In all, 100 μL of the purified activated SOD and 50 μL of the purified activated antibody (either targeting anti-NR1 or control rabbit anti-bovine) were then mixed

with 1 mL of PBCA nanoparticle suspension. This mixture was incubated in the dark for 40 minutes and then transferred into a 12-well plate and exposed to UV irradiation for 20 minutes (1 cm distance, $\lambda = 360$ nm, 16 W) using a Spectroline UV lamp (Westbury, NY, USA). The mixture was stirred every 5 minutes during the UV exposure, and was then collected on its completion into a 2-mL centrifuge tube and stored overnight at 4°C. The free enzyme was then removed by centrifugation (4,500 r.c.f., 30 minutes) followed by resuspension in 1 mL of 20 mmol/L HEPES buffer. Centrifugation/resuspension procedure was repeated twice to ensure complete removal of unconjugated enzyme. Binding yield for antibody attachment was determined using AlexaFluor 594-labeled antibody, as described previously.[31]

Protein attachment to liposomes. Superoxide dismutase and anti-NR1 or control antibody were first mixed with the Traut's reagent and incubated for 1 hour in the dark in an incubator shaker at room temperature to introduce thiol groups. Where applicable, fluorescent labeling of proteins by AlexaFluor 594 dye was performed simultaneously with the protein activation by the Traut's reagent. After incubation, the excess of the Traut's reagent was removed by microfiltration using 30 kDa MWCO centrifugal devices for anti-NR1 antibody, and 10 kDa MWCO centrifugal devices for SOD. Activated proteins were then mixed with maleimide-terminated liposomes and incubated overnight at room temperature on gentle shaking. In all, 2.5 mg of SOD and 100 μg of the antibody, respectively, were used for the preparation of 1 mL of the liposomal suspension. Unattached proteins were removed by dialysis against 20 mmol/L HEPES buffer for 48 hours, using Biotech Cellulose Ester (CE) Dialysis Membranes (MWCO: 300,000, diameter: 10 mm). Finally, protein-coated liposomes were filtered through 0.2 micron filter to achieve sterilization and to remove large aggregates. Binding yield for antibody attachment was determined using AlexaFluor 594-labeled antibody.

Synthesis of bulk-loaded poly(lactide-co-glycolide) nanoparticles. The SOD-incorporated-PLGA NPs were manufactured using a double emulsion solvent evaporation technique, as described by Reddy *et al*.[27,28] First, fluorescently labeled SOD was prepared by dissolving 2 mg of SOD (6,000 U) in 300 μL of HPLC-grade water and adding 20 μL of AlexaFluor495 solution in dimethylformamide, followed by incubation at room temperature for 60 min with gentle shaking. Unbound dye was removed by centrifugation through a Microsep centrifugation device (10 kDa MWCO). Labeled SOD was reconstituted in 30 μL of HPLC-grade water and mixed with a solution of 3 mg RSA in 30 μL of HPLC-grade water. This 60 μL aqueous solution containing both SOD and RSA was mixed with the solution of 15 mg of PLGA in 0.5 mL of chloroform. The mixture was first vortexed for 1 minute, and then emulsified using a microtip probe sonicator (Omni Ruptor 4000) at 30 W of energy output to form a stable water-in-oil emulsion. Sonication was stopped immediately after achievement of uniform distribution of fluorescent aqueous phase (containing AlexaFluor-labeled SOD) in chloroform phase. Sonication time at this step was critical for the preparation of NPs with high SOD incorporation yield. If undersonicated, then the emulsion lacked homogeneity, while oversonication led to chloroform evaporation and protein precipitation form the liquid phase even when a cooling ice bath was used. Optimal sonication time differed considerably from batch to batch; however, we found that use of fluorescently labeled SOD (the only modification compared with the method described) enabled us to visually control homogenization process helping to avoid precipitation.[27,28] The uniform water-in-oil emulsion was further emulsified into 2 mL of aqueous solution containing 5% w/v polyvinyl alcohol by vortexing followed by sonication, as described above. The double emulsion was shaken overnight in an open 15 mL centrifugation tube in incubator at room temperature to evaporate chloroform. The polyvinyl alcohol and unincorporated proteins were removed by centrifugation (4,500 r.c.f., 30 minutes) and purified nanoparticles were resuspended in 1.2 mL of HPLC-grade water. This centrifugation and resuspension cycle was repeated three times. Finally, the suspension was reconstructed in 0.5 mL of phosphate-buffered saline buffer. Antibody attachment to the surface of the nanoparticles was performed using Sulfo-NHS-LC-Diazirine crosslinker as described above for PBCA nanoparticles. Using the procedure described above, we were able to reproducibly prepare SOD-loaded PLGA NPs with total SOD activity $>2{,}000$ U/mL (Supplementary Table 1), which was considerably higher than that reported (~ 200 U/mL).[27,28]

Analysis of superoxide dismutase activity. Activity of SOD was measured using an SOD assay Kit (Sigma-Aldrich Corporate life science). This assay is based on using a highly water-soluble tetrazolium salt, WST-1 (2-(4-Iodophenyl)-3-(4-nitrophenyl)-5-(2,4-disulfophenyl)-2H-terazolium, monosodium salt) which would produce a water soluble formazan dye (WST-1 formazan) on interaction with superoxide. Superoxide is generated by xanthine oxidase/xanthine system. The rate of the production of WST-1 formazan dye is linearly related to the concentration of the generated superoxide, which is reduced by SOD. Colorimetric method is used for detection since WST-1 is colorless while WST-1 formazan has characteristic absorption maximum at 450 nm.

A 20-μL aliquot of each sample ($n = 3$) was added to a 96-well plate, followed by addition of the assay reagents. The plate was incubated at 37°C for 40 minutes, and the absorbance at 450 nm was read using a Synergy HT Multi-Mode Microplate Reader (Bio-Tek Instruments, Inc., Winooski, VT, USA). The standard plot (0.1 to 100 U/mL) was prepared by diluting known SOD concentrations in the dilution buffer provided by the manufacturer of the assay. The inhibition rate was calculated according to the following equation:

$$\text{Inhibition rate } \% = (((\text{Ablank } 1 - \text{Ablank } 3) - (\text{Asample} - \text{Ablank } 2))/(\text{Ablank } 1 - \text{Ablank } 3)) \times 100\%.$$

Since the most accurate determination of SOD activity occurs for SOD concentrations between 1 and 20 U/mL, all in samples with unknown SOD activity were diluted before performing the activity assay so that their activity was in this range.

When measuring SOD activity for bulk-loaded PLGA samples we characterized both 'surface' activity, which was measured for freshly prepared SOD-loaded nanoparticles, and 'total' activity, which was measured after dissolution of PLGA nanoparticles and therefore corresponded to all SOD loaded in PLGA. In the latter case, bulk-loaded nanoparticles were freeze-dried and dissolved in 0.5 mL of chloroform followed by adding 0.5 mL of phosphate-buffered saline buffer. The mixture was then incubated for 1 hour on shaking to extract water-soluble components. In all, 20 μL aliquot was then collected from the aqueous phase using a 100-μL pipettor and used after further dilution to measure SOD activity.

Particle size analysis and zeta potential. The hydrodynamic diameter of NPs and liposomes was measured using dynamic light scattering. A transparent cuvette was filled with 3 mL of HPLC-grade water followed by adding 10 μL of the sample. Then, suspension was carefully mixed by a pipette with special attention paid to avoid formation of the bubbles. The capped cuvette was placed in a 90 Plus Particle Size Analyzer (Brookhaven Instruments Corporation, Holtsville, NY, USA) and the dynamic light scattering data were read for 30 minutes (10 runs, 3 minutes per run). Zeta potential was also measured using the 90 Plus Particle Size Analyzer.

Lyophilization and accelerated aging experiment. Sucrose and trehalose were used as cryoprotectors. Concentrated stock solutions of cryoprotectors (1 g/mL) were prepared in advance and mixed with the samples in 1:9 volume ratio to achieve final concentration of the cryoprotector of 100 mg/mL, or 10% (w/v). Samples were frozen overnight at -80°C before being lyophilized for 48 hours.

To shorten the duration of the aging experiment, 37°C incubation was used to achieve an aging rate ~ 3 times faster than at room temperature. Although higher temperatures (e.g., 50°C) are often used for accelerated aging studies, these were not suitable for studies involving PLGA NPs, because PLGA glass transition temperature is close to 40°C, and for liposomes, because they tend to degrade above 40°C. Thus, all accelerated aging experiments were performed at 37°C. Incubation was stopped at different time points (2, 7, 15, 30, 60, and 120 days), and the SOD activity of the samples was measured for resuspended samples and compared with that of the same samples immediately after preparation.

Animal Studies

Animals. C57BL/6 mice (Harlan Laboratories, Indianapolis, IN, USA), weighing 22 to 25 g each were given free access to food and water before the experiment. All animal experiments were approved by the Ralph H Johnson VA Medical Center IACUC and followed NIH and ARRIVE guidelines.

Administration of nanoparticles. Animals were subjected to 1 hour ischemia followed by 1 hour or 24 hours reperfusion.[34,35] Animals were randomly assigned to a control group ($n = 12$) or groups ($n = 12$) treated with an intracartoid injection of nanoparticles at 25 U of SOD activity per

injection. Nanoparticles or liposomes were prepared as described above and the solution was stored at 4°C. Control groups received nanoparticles or liposomes without SOD. The bolus intracartoid injections were given immediately after the onset of reperfusion or at various times after reperfusion.[28]

Induction of ischemia. The animals were anesthetized with halothane (1% in 70%/30% NO_2/O_2 by mask). Monitoring of mean arterial blood pressure via tail cuff apparatus, and blood samples were collected to determine arterial pH levels and $PaCO_2$ and PaO_2. The mean arterial blood pressure and heart rate were recorded using a Visitech System blood pressure monitor (Apex, NC, USA). Brain temperature was monitored using a rectal thermometer and thermistor probe inserted into the temporalis muscle. The animals' body temperature was maintained at 37°C by using a water-jacketed heating pad. Brain temperature was monitored for 1 hour before ischemia to 6 hours after ischemia and was recorded at 30-minute intervals. Each mouse was anesthetized and the external carotid artery (ECA) and common carotid artery were isolated.[36,37] The left common carotid artery was exposed through a midline incision in the neck. The superior thyroid and occipital arteries were electrocoagulated and divided. A microsurgical clip was placed around the origin of the ECA. The distal end of the ECA was ligated with 6-0 silk and transected. A 6-0 silk was tied loosely around the ECA stump. The clip was removed and the fire-polished tip of a 5-0 nylon suture (silicone coated) was gently inserted into the ECA stump. The loop of the 6-0 silk was tightened around the stump and the nylon suture was advanced $\sim$13 mm (adjusted for body weight) into and through the internal carotid artery until it rested in the anterior cerebral artery, thereby occluding the anterior communicating and middle cerebral arteries. After the nylon suture was in place for 1 hour, it was pulled back into the ECA and the incision closed.

Enzyme-linked immunosorbent assay analysis. For quantitative analysis of cytokines, an enzyme-linked immunosorbent assay was used to measure the levels of tumor necrosis factor-α, interleukin-1β, or transforming growth factor-β in brain tissue. Cytokines were extracted from mouse brains as follows: frozen hemibrains were placed in Tissue Homogenization Buffer containing Protease Inhibitor Cocktail (PIC, Sigma, St Louis, MO, USA) 1:1,000 dilution immediately before use, and homogenized using polytron. Tissue sample suspensions were distributed in aliquots and snap frozen in liquid nitrogen for later measurements. Invitrogen ELISA kit was then used, according to manufacturer directions.

Histologic examination. For histologic examination, the animals were anesthetized with an intraperitoneal injection of sodium pentobarbital (50 mg/kg) 24 hours after induction of ischemia. Mice brains were transcardially perfused with 4°C, 10% phosphate-buffered saline. The brains were then removed and chilled for 15 minutes at -20°C before being placed in a Rodent Brain Matrix. Cronal sections (1-mm thickness) were prepared and subjected to 2% triphenyltetrazolium chloride (TTC) staining at 37°C.[9,10] The TTC stains live tissue (red) versus dead or dying tissue (white). Seven serial one-mm thick coronal sections through the rostral to caudal extent of the infarction were obtained from each brain, beginning 2 mm from the frontal pole. The TTC-stained sections were placed in 10% neutral buffered formalin and kept in darkness at 4°C for at least 24 hour. The infarct area in each section was determined with a computer-assisted image analysis system, consisting of a Power Macintosh computer equipped with a Quick Capture frame grabber card, Hitachi CCD camera mounted on an Olympus microscope and camera stand. NIH Image Analysis Software, v. 1.55 (NIH, Bethesda, MD, USA) was used. The images were captured and the total area of damage determined over the seven sections. A single operator blinded to treatment status performed all measurements. The infarct volume was calculated by summing the infarct volumes of the sections. Infarct size (%) was calculated by using the following formula: (contralateral volume $-$ ipsilateral undamaged volume) $\times$ 100/contralateral volume to eliminate effects of edema.

Measurement of cerebral blood flow. Cerebral blood flow (CBF) was monitored by using a laser Doppler flowmeter.[36] The CBF values were determined as a percentage, because the values displayed by the laser Doppler flowmeter were not absolute. As described above, the animals were anesthetized with halothane (1% in 70%/30% NO_2/O_2 by mask) and were mounted in a stereotaxic frame and the probes were fixed to the head. In the hemisphere ipsilateral to the middle cerebral artery occlusion, coordinates were as follows: point A, 0.5 mm posterior to the bregma and 2 mm lateral to the midline; point B, 1 mm posterior to the bregma and 1.2 mm lateral to the midline; point D, 1 mm anterior to the bregma and 1.7 mm lateral to the midline; and point C in the contralateral hemisphere, 1 mm posterior to the bregma and 2 mm from the midline. Cerebral blood flow was compared at 15 minutes before the onset of ischemia, during ischemia (15 minutes after the start of ischemia) before injection of test particles, and at 30 minutes after injection (continuous measurements were taken from 15 minutes before ischemia to 30 minutes after the end of injection of the compound). Animals were reanesthetized and the CBF was measured at 3 hours after reperfusion. The mean values before middle cerebral artery occlusion were taken as baseline and the data thereafter were expressed as percentages of the baseline value.

Behavioral assessment. Behavioral tests (neurologic deficit) were performed before and after ischemic injury.[36] Neurologic scores were as follows: 0, normal motor function; 1, flexion of torso and contralateral forelimb when animal was lifted by the tail; 2, circling to the contralateral side when held by tail on flat surface, but normal posture at rest; 3, leaning to the contralateral side at rest; 4, no spontaneous motor activity.

Thiobarbituric acid reactive substances. LPO (lipoperoxidation) was evaluated by thiobarbituric acid reactive substances (TBARS) test.[38] Aliquots of samples were incubated with 10% trichloroacetic acid and 0.67% thiobarbituric acid. The mixture was heated (30 minutes) on a boiling water bath. Afterwards, n-butanol was added and the mixture was centrifuged (1,000 $\times$ *g* for 10 minutes). The organic phase was collected to measure fluorescence at excitation and emission wavelengths of 515 and 553 nm, respectively. 1,1,3,3-tetramethoxypropane, which is converted to MDA (malondialdehyde), was used as standard. Results are expressed as pmol MDA/mg protein and reported as percentage of control.

Free radical levels. To assess the free radicals content, we used 2′-7′-dichlorofluorescein diacetate (DCFH-DA) as a probe.[39,40] A sample aliquot was incubated with DCFH-DA (100 μM) at 37°C for 30 minutes; the reaction was terminated by chilling the reaction mixture in ice. The formation of the oxidized fluorescent derivative (DCF) was monitored at excitation and emission wavelengths of 488 and 525 nm, respectively, using a fluorescence spectrophotometer (Hitachi F-2000, Hitachi High-Tech, Northridge, CA, USA). The free radicals content was quantified using a DCF standard curve and the results were expressed as pmol of DCF formed/mg protein. All procedures were performed in the dark and blanks containing DCFH-DA (no homogenate) were processed for measurement of autofluorescence.[28]

Superoxide dismutase activity. Activity of SOD was determined using a RANSOD kit (Randox Labs, Kearneysville, WV, USA). This method uses xanthine and xanthine oxidase to generate O_2 that reacts with 2-(4-iodophenyl)-3-(4-nitrophenol)-5-phenyltetrazolium chloride to form a red formazan dye, which is assayed spectrophotometrically at 505 nm at 37°C. The inhibition of chromogen production is proportional to SOD activity present in the sample.

Protein determination. Protein was measured by the Coomassie blue method using bovine serum albumin as standard.

Neuronal cultures. Cortical tissues dissected from C57BL/6 mouse embryos at the E18 developmental stage were incubated for 15 minutes in a solution of 2 mg/mL trypsin in Ca^{2+}/Mg^{2+}-free Hank's balanced salt solution (HBSS) (Invitrogen) buffered with 10 mmol/L HEPES. Tissues were then dissociated and the cells were plated in 60 or 100-mm diameter plastic dishes or 24-well plates and maintained at 37°C in Neurobasal medium containing B-27 supplements (Invitrogen), 2 mmol/L L-glutamine, 0.001% gentamycin sulfate, and 1 mmol/L HEPES (pH 7.2). Experiments were performed in 7- to 9-day-old cultures. Approximately 95% of the cells in such cultures were neurons and the remaining cells were astrocytes. For OGD, neurons were incubated in glucose-free Locke's medium in an oxygen-free chamber with 95% N2/5% CO_2 atmosphere for 24 hours. Effects of nanoparticles with and without SOD against glucose deprivation or OGD-induced neuronal cell death were determined by trypan blue dye exclusion assay.

Statistical Analysis

The results were expressed as the mean $\pm$ standard deviation (s.d.). The statistical significance of the results in infarct volume, neurologic deficit,

physiologic and histologic data was analyzed using a one-way analysis of variance (ANOVA) followed by Fisher's *post hoc* test.

RESULTS

Preparation of Nanoparticles

Supplementary Table 1 provides information about nanoparticle size, SOD activity, and antibody binding yields for PBCA NPs, liposomes, and bulk-loaded PLGA NPs, respectively. The hydrodynamic radius of the liposomes was found to be almost twice as small as that for PBCA and PLGA NPs, making possible their sterilization using 0.2 μm filters. Alternative sterilization method (1 hour UV irradiation, 1 cm distance, $\lambda = 360$ nm, 16 W lamp) was used in the case of PBCA and PLGA NPs. All the liposomes and NPs made in this study had highly negative zeta potentials varying from -45 to -65 mV, indicating high stability of colloidal suspensions. Presence or absence of either anti-NR1 or control antibody did not have any statistically significant effect on the size or zeta potential of NPs or liposomes ($P > 0.05$). The SOD activity of the liposomes was just below 2,000 U/mL (see Supplementary Table 1) and was similar to that of PBCA NPs. Total activity of PLGA NPs obtained after degradation of PLGA NPs and release of all loaded SOD (>4,000 U/mL) was higher than that of the liposomes and PBCA NPs probably because of better SOD loading yield. As expected, 'current' activity of PLGA NPs was much lower and consisted of ~150 to 200 U/mL because only a small fraction of SOD loaded in PLGA is available on the surface. Total SOD activity was used to calculate the dose for *in vivo* experiments. Presence or absence of an antibody did not have effect on SOD activity of the samples ($P > 0.05$). Binding efficiency of anti-NR1 and control antibody for different delivery vehicles is also shown in Supplementary Table 1. For the same antibody, binding yields and final antibody concentrations were different for different delivery vehicles (ANOVA, $P < 0.05$). Therefore, different delivery vehicles had same SOD activity (25 U) but different concentrations of the targeting anti-NR1 antibody in our *in vivo* experiments.

Lyophilization and Shelf-Life

Size, zeta potential, and activity of liposomes and NPs before and after lyophilization are shown in Supplementary Table 2. If no cryoprotector was used, then lyophilization resulted in decreased SOD activity and increased mean hydrodynamic diameter, probably because of partial aggregation of the carriers. However, we found that use of trehalose or sucrose as a cryoprotector prevented increase in the diameter and improved SOD activity of the vehicles after lyophilization. Based on the activity data (Figure 1A; Supplementary Table 2), sucrose appears to offer better cryoprotection than trehalose.

The activity of SOD-coated liposomes lacking an antibody after long-term storage at 37°C is shown in Figure 1B. In this experiment, we compared stability of the liposomes stored in colloidal suspension to that of the liposomes freeze dried with a cryoprotector. The samples that were stored as colloidal suspensions lost more activity than their freeze-dried counterparts. The lyophilized SOD liposomes retained ~80% of the original activity after 120 days of incubation at 37°C, which corresponds to ~1 year shelf-life at room temperature. At the same time, non-lyophilized liposomes retained ~60% of activity ($P < 0.05$).

Neuronal Cell Culture Studies

Neuronal cortical cell cultures were established from day 18 embryos and grown for 7 to 10 days on poly-L-lysine coated dishes. The cells were exposed to OGD for 24 hours. At the time of OGD, the cells were incubated in the presence of nothing or nanoparticles (PBCA) with and without SOD/antibody. At the end of the incubation period, the cell viability was quantified by a Trypan blue exclusion assay. The results of these experiments

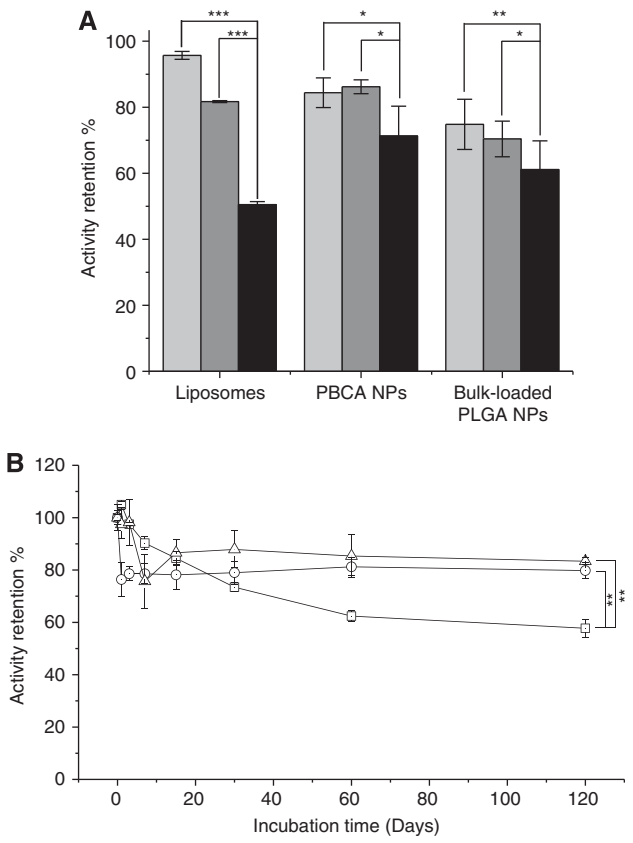

Figure 1. Effect of freeze drying and cryoprotecting additives on superoxide dismutase (SOD) activity of SOD NP conjugates and shelf-life study for SOD liposomes. (**A**) Activity of freshly prepared conjugates before freeze drying was considered to be 100%. Sucrose is preferred cryoprotector because its use leads to the highest activity retention for all types of conjugates. All conjugates here are lacking the antibody. Cryoprotector control (black); sucrose (light gray) and trehalose (dark gray). (**B**) For samples with sucrose and trehalose cryoprotectors, ~80% of activity is retained after 120 days of accelerated aging at 37°C, which corresponds to ~1 year shelf-life on storage at room temperature. SOD activity immediately after freeze drying was considered to be 100%. All conjugates here are lacking the antibody. SOD liposomes without any cryoprotector (square); SOD liposomes with sucrose (circle) and trehalose (triangle). *$P < 0.01$, **$P < 0.05$, ***$P < 0.001$. PLGA, poly(lactide-co-glycolide).

indicate that nanoparticles with SOD could protect the neuronal cells from the toxicity of OGD (Figure 2). The percent surviving cells were saline—34.89 ± 7.47; PBCA—33.03 ± 4.06; PBCA-SOD—60.45 ± 7.97; PBCA-SOD-Ab—76.46 ± 5.45; PBCA-SOD-NR1—84.96 ± 5.99. The presence of the antibodies showed an increased protective effect, while the different antibodies did not make a difference in the protective effect *in vitro*. In the absence of SOD, the cells underwent apoptosis.

Cerebral Ischemia-Reperfusion Injury in the Mouse

To determine if the nanoparticles would enter the brain after cerebral ischemia and reperfusion injury, we injected the fluorescently labeled nanoparticles through the carotid artery (intracartoid) as previously shown to be effective.[28] Figure 3 shows the effect of injection of PBCA nanoparticles into the brain. Animals were subjected to cerebral ischemia (1 hour) and reperfusion injury (1 hour) with fluorescent nanoparticles injected at the beginning of the reperfusion period. The efficiency of uptake of the nanoparticles into the brain was determined by the

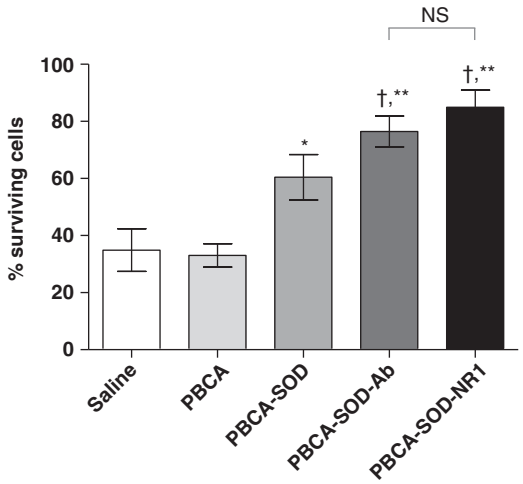

Figure 2. Primary neuronal cells incubated with glutamate and treated with saline or PBCA nanoparticles (NPs). NPs were added at the same time as oxygen-glucose deprivation (OGD) and incubated for 24 hours. The cells were then assayed using a trypan blue exclusion dye method. Random areas were selected and the numbers of dead/live cells were determined and the % surviving cells plotted against treatment. A total of 1,000 cells were counted. $^{*}P<0.01$, compared with saline and PBCA; $^{\dagger}P<0.01$, compared with PBCA SOD; $^{**}P<0.001$, compared with saline and PBCA. Saline, no nanoparticles; PBCA, nanoparticles alone; PBCA-SOD, PBCA nanoparticles with SOD; PBCA-SOD-Ab, PBCA nanoparticles with SOD and nonspecific antibody; PBCA-SOD-NR1, Ab, non-specific antibody; PBCA nanoparticles with SOD and NR1 antibody. $N=6$ repeats of 4 cultures each. PBCA, polybutylcyanoacrylate; NMDA, *N*-methyl-D-aspartate; NR-1, NMDA receptor antibody; SOD, superoxide dismutase.

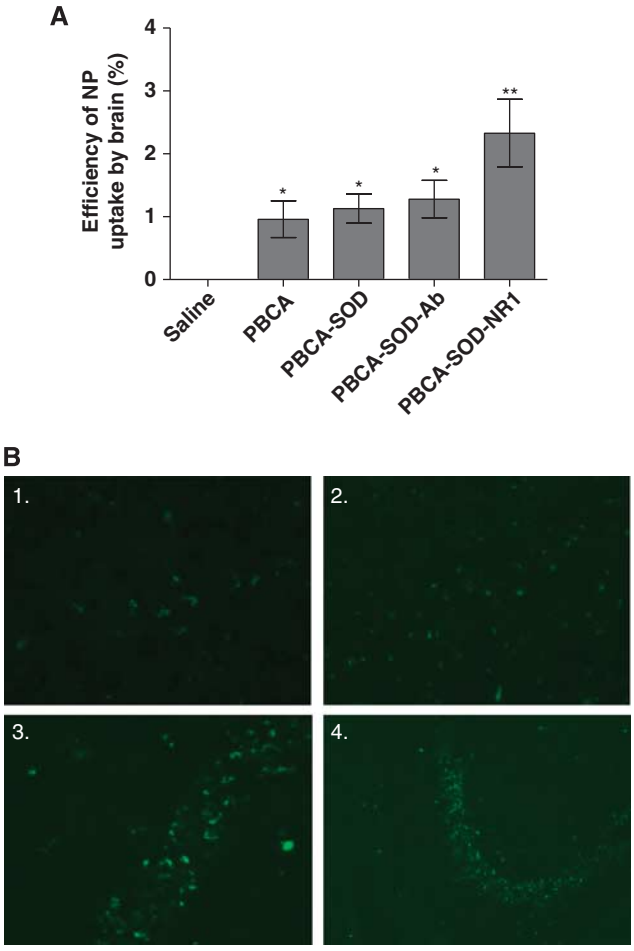

Figure 3. Efficiency of uptake of polybutylcyanoacrylate (PBCA) nanoparticles (NPs) in the brain after cerebral ischemia and reperfusion injury. Animals were made ischemic and injected with PBCA nanoparticles and examined for the efficiency of uptake into the brain. (**A**) The percent nanoparticles in the brain were determined by quantifying the fluorescent nanoparticles. (**B**) Pictures of brains with nanoparticles. 1 and 2, PBCA-SOD-Ab particles; 3 and 4, PBCA-SOD-NR1 particles. $N=10$ per group. $^{*}P<0.01$; $^{**}P<0.001$. Ab, non-specific antibody; NMDA, *N*-methyl-D-aspartate; NR-1, NMDA receptor antibody; PBCA, polybutylcyanoacrylate; SOD, superoxide dismutase.

amount of fluorescence present after injection. Injection of the nanoparticles showed that the targeted nanoparticles were taken up into the brain to a greater efficiency than the nontargeted particles (Figure 4A, saline, 0.0 ± 0.00; PBCA, 0.96 ± 0.29; PBCA-SOD, 1.13 ± 0.23; PBCA-SOD-Ab, 1.28 ± 0.30; PBCA-SOD-NR1, 2.33 ± 0.54). PBCA and PBCA-SOD-Ab fluorescent particles showed fluorescence in the brain but with a nonspecific distribution (Figure 3B1 and 3B2, respectively), while PBCA-SOD-NR1 showed both nonspecific and specific distribution of the nanoparticles (Figure 3B3 and 3B4). The PBCA-NR1 localized to the CA region of the hippocampus as indicated in Figure 3B4. Better penetration and specificity may have been enhanced by the presence of the NR1 antibody on the nanoparticles. The intracartoid injection of SOD alone did not show penetration into the uninjured brain (data not shown).

To determine the effect of nanoparticles on protection from ischemic injury, mice were subjected to 1 hour of ischemia followed by 24 hours of reperfusion. Nanoparticles were administered intracartoid at the start of reperfusion, to ensure maximum protection (Figure 4). Compared with the saline-injected group, the infarct volume in the brains was not decreased in the brains of animals treated with the PBCA nanoparticles alone (Figures 4A and 4B; saline (Figure 4A1), $64.07 \pm 8.34\,mm^3$; PBCA (Figure 4A2), $62.15 \pm 6.19\,mm^3$). The infarct volume was significantly decreased in all of the groups treated with PBCA nanoparticles in the presence of SOD (Figures 4A and 4B; PBCA-SOD (Figure 4A3), $41.81 \pm 7.74\,mm^3$; PBCA-SOD-Ab (Figure 4A3), $38.09 \pm 9.54\,mm^3$; PBCA-SOD-NR1 (Figure 4A4), $24.64 \pm 6.65\,mm^3$), suggesting that the SOD-coated nanoparticles were efficient at traversing the BBB and eliciting an effect on free radicals generated by the ischemia and reperfusion injury. The PBCA-SOD-NR1 nanoparticles showed better protection from the ischemia and reperfusion injury than the PBCA-SOD-Ab nanoparticles. Injection of native SOD (without nanoparticles) showed no protection (data not shown). Assessment of behavior showed that the SOD-coated nanoparticles showed a significant improvement over the control nanoparticles, with the NR1-coated particles showing an appreciably better improvement (saline, 2.10 ± 0.23; PBCA, 2.0 ± 0.21; PBCA-SOD, 1.60 ± 0.22; PBCA-SOD-Ab, 1.40 ± 0.16; PBCA-SOD-NR1, 0.800 ± 0.20). In addition, survival rate was determined in the animals treated with the PBCA nanoparticles (Figure 4D). Notably, PBCA-NR1 controls lacking SOD did not show any therapeutic efficacy (data not shown), indicating that effect of NR1 antibody was likely because of targeting rather than because of reducing glutamatergic toxicity. Finally, the various nanoparticles (liposomes, polylactic acid, and PLGA) were examined for effects on infarct volumes in the mice after ischemia and reperfusion injury (Figure 4E). In all treatment groups, targeted nanoparticles coated by NR1 antibody showed a significant improvement over the nontargeted nanoparticles. All three delivery vehicles showed similar effect on the infarct volumes. There were no significant differences in measured physiologic parameters (Supplementary Table 3; mean arterial pressure, blood pO_2, pCO_2, CBF, and pH)

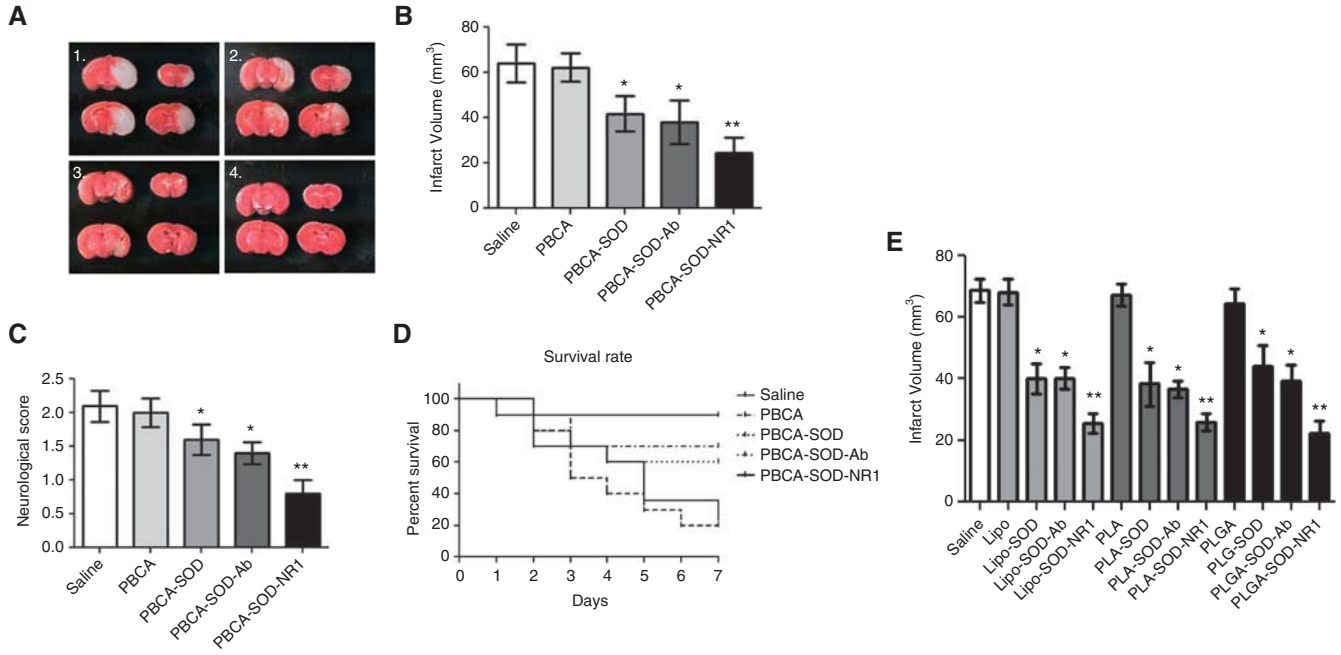

Figure 4. Effect of nanoparticles on infarct volume, neurologic score, and survival rate in mice subjected to ischemia and reperfusion injury (IRI). Mice were subjected to 1 hour ischemia and 24 hours of reperfusion with treatment of PCBA particles immediately after ischemia. (**A**) Brains stained with triphenyltetrazolium chloride (TTC) after IRI for infarct volume. 1. PBCA; 2. PBCA-SOD; 3. PBCA-SOD-Ab; 4. PBCA-SOD-NR1. (**B**) Quantification of infarct volumes from animals in (**A**). (**C**) Neurologic score from IRI mice at 22 hours after reperfusion and treatment. (**D**) Percent survival of mice after IRI and nanoparticle treatment. Saline or PBCA-treated mice were followed for up to 7 days after treatment. $N = 10$ per group. $^{*}P < 0.05$; $^{**}P < 0.01$. (**E**) Mice were subjected to 1 hour ischemia and 24 hours of reperfusion. Immediately after ischemia, animals were administered nanoparticles and infarct volumes determined at 24 hours. $N = 10$ per group. $^{*}P < 0.01$; $^{**}P < 0.01$ compared with SOD and SOD-Ab for each group. Lipo, liposomes; PLA, polylactic acid; PLGA, poly (lactic-co-glycolic acid). Ab, non-specific antibody; NMDA receptor antibody; NR-1, NMDA, *N*-methyl-D-aspartate; PBCA, polybutylcyanoacrylate; SOD, superoxide dismutase.

between the vehicle and treated mice at baseline, during ischemia, or after reperfusion. As seen in the table, the CBF measurements were not altered by the presence of the various nanoparticles. In addition, after ischemic injury the CBF decreased to 20% and after reperfusion returned to ~90% in all treatment groups.

To determine the neuroprotective mechanism of action of the nanoparticles in the mouse brain after ischemic injury, animal brains were examined for the expression of inflammatory mediators. We determined the levels of the cytokine tumor necrosis factor-α, interleukin-1β, and transforming growth factor-β at 24 hour after ischemic injury (Figure 5). As seen in the figure, the PBCA nanoparticles with SOD significantly reduced tumor necrosis factor-α, interleukin-1β, and transforming growth fact-β levels after ischemic injury. The PBCA-SOD-NR1 nanoparticles showed the greatest effect reducing the above cytokine levels by 74%, 86%, and 85%, respectively.

Administration of the PBCA nanoparticles containing SOD revealed changes in DCF measurements in the ipsilateral hemisphere after ischemic injury resulting in a decrease in free radicals compared with the animals treated by saline or PBCA alone (Figure 5D). The PBCA-SOD-NR1 nanoparticles showed the greatest improvement with a 76% reduction in free radicals. The PBCA nanoparticles showed an effect on TBARS levels in the brain after ischemia and reperfusion injury (Figure 5E). Significant differences were present in the lesion area with all the SOD nanoparticles demonstrating some effect in reducing lipid peroxidation products after ischemic injury. *Post hoc* test showed that the saline and PBCA-treated ischemic mice had greater values as compared with the other groups. No significant differences were present in the saline or PBCA samples. However, the PBCA-SOD-NR1 nanoparticles showed a 77% reduction in TBARS. Finally, to determine if these changes were because of increased SOD activity provided by the nanoparticles, we measured SOD activity in the brains of the mice after ischemia and reperfusion injury (Figure 5F). There were differences in SOD activity in the brains of the various groups. Analysis showed lower values for ischemic mice injected with saline or PBCA as compared with the other groups (Figure 5F). Mice treated with SOD nanoparticles showed a significant increase in SOD activity with the PBCA-SOD-NR1 showing the greatest increase (~2× over control).

A consistent result for caspase-3 activity was detected in different groups. We found that middle cerebral artery occlusion produced a significant increase in caspase-3 activity in the ipsilateral injured cortex at 24 hours after injury, and the SOD nanoparticles reduced the caspase-3 activity compared with the vehicle-treated animals. The dose of nanoparticles caused a reduction in caspase-3 activity at 24 hours after reperfusion (Figure 5H). Again, targeted NR1-SOD nanoparticles were most efficient in reducing caspase-3 activity. These results confirmed that the mitochondrial-dependent apoptotic pathway was activated during reperfusion, and the SOD nanoparticles actively suppressed caspase-3 activation.

To determine the time course of protection afforded by the PBCA-SOD-NR1 in the mouse model of ischemia and reperfusion injury, we further examined the effects of the nanoparticles after administration at different times after the start of reperfusion. Mice were subjected to 1 hour of ischemia and 48 hours of reperfusion for assessment. Animals were treated with PBCA-SOD-NR1 nanoparticles at 1, 2, 4, 8, and 24 hours after the end of the ischemic period and examined for infarct volumes (Figure 6). Post ischemia intracartoid administration of the nanoparticles reduced the infarct volume in the animal brains: Nanoparticles administered at 1, 2, 4, and 8 hours after ischemia showed 65%, 59%, 44%, and 23% lesion area compared with the control animals, respectively. The infarct volume of the animals treated at 24 hours

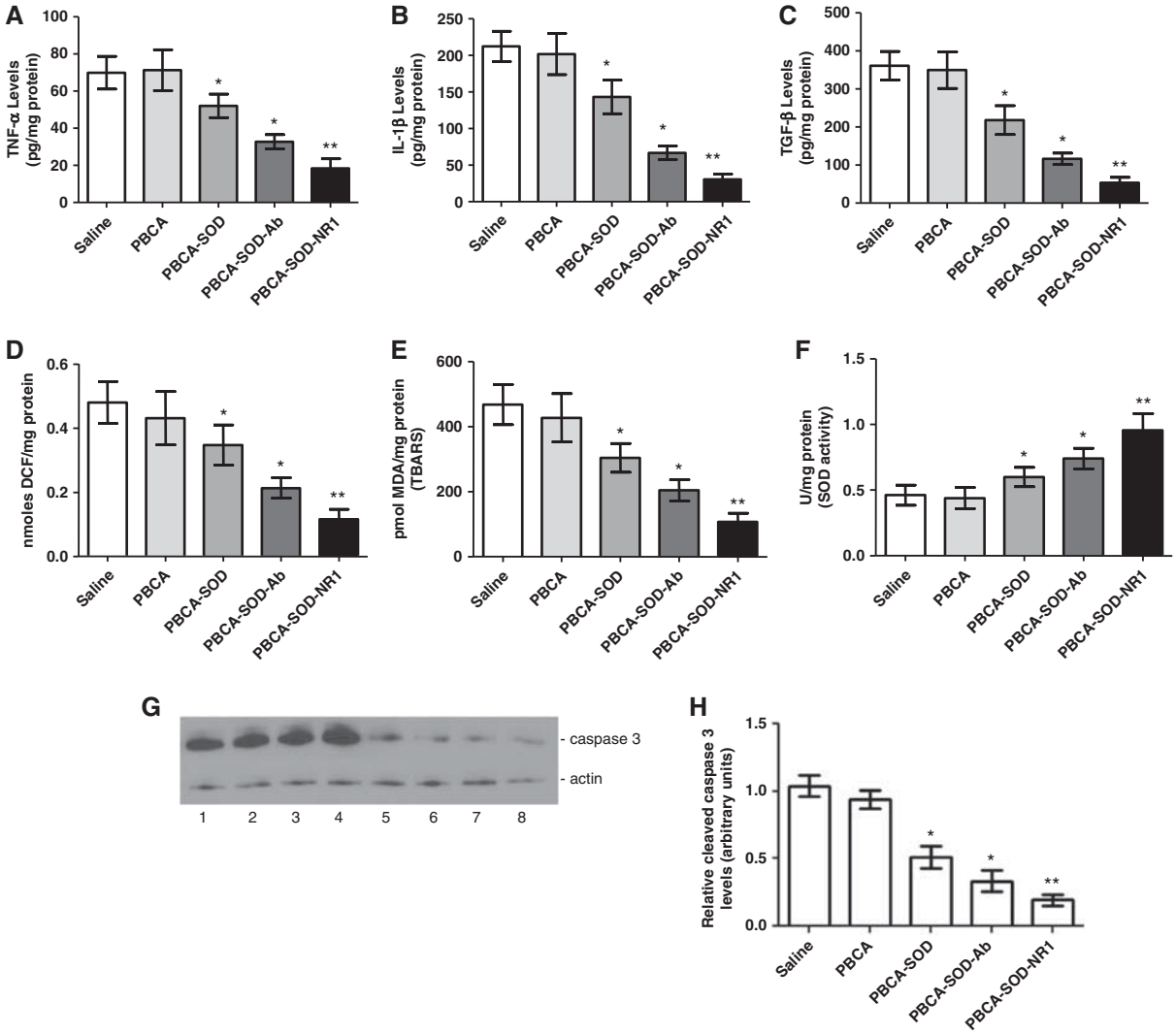

Figure 5. Reduced inflammatory markers, free radical levels, thiobarbituric acid reactive substances (TBARS), superoxide dismutase (SOD) activity and caspase 3 activation in the brain after ischemia. The following inflammatory markers were measured in mice after ischemia and reperfusion injury: (**A**) tumor necrosis factor-α (TNF-α); (**B**) interleukin-1β (IL-1β); and (**C**) transforming growth factor-β (TGF-β). Mice were subjected to 1 hour of ischemia, treated with polybutylcyanoacrylate (PBCA) nanoparticles and followed by 24 hours of reperfusion. Quantitative analysis of cytokines in the ischemic brain was determined by enzyme-linked immunosorbent assay (ELISA). (**D**) Free radicals content was detected using 2′-7′-dichlorofluorescein diacetate (DCFH-DA) on tissue homogenates. (**E**) TBARS were assayed as described in Materials and methods. (**F**) SOD activity was determined in mice at the end of the study to measure the effect of nanoparticle delivered SOD on the outcome from ischemic injury. $N = 10$ per group. (**G**) Mice were subjected to ischemia and reperfusion injury followed by PBCA or PBCA/SOD nanoparticles at the end of ischemic injury. Animals were killed at 24 hours and the brain homogenates subjected to western blot analysis for active caspase 3 and β actin. Lanes 1 to 4, PBCA nanoparticles; lanes 5 to 8, PBCA-SOD-NR1 nanoparticles. (**H**) Quantitation of western blots. $N = 10$ per group. *$P < 0.01$; **$P < 0.001$. Ab, non-specific antibody; NR-1, *N*-methyl-D-aspartate; NMDA receptor antibody; NMDA.

after ischemia did not reach statistical significance from the vehicle-treated animals.

DISCUSSION

The aim of this study was to determine the impact of targeted nanoparticle delivery of SOD on protection from ischemia and reperfusion injury in the brain. In the present study, we used various nanoparticle delivery systems to administer SOD to the brain. The studies showed that targeted SOD nanoparticles with NR1 antibody reduced the infarct lesion in the mouse model of cerebral ischemia and reperfusion injury. The study also showed a significant improvement in neurologic function and survival, as well as a reduction in inflammatory markers. Furthermore, there was a reduction in oxidative stress and apoptotic markers in the brain after treatment. Finally, there was clinically relevant time window for administration of the targeted nanoparticles to provide an opportunity for treatment.

A number of studies have shown that SODs are the major antioxidant enzymes.[41,42] These include copper/zinc SOD (SOD1, cytosolic), manganese SOD (SOD2, mitochondrial), and extracellular SOD (ECSOD, extracellular) and account for $\sim$0.1% of the total protein in the cell.[9] Studies have shown that SOD1 transgenic mice are protected from ischemia and reperfusion injury while SOD1- and SOD2-deficient mice have increased cell death.[41–44] SOD1 has been used in experimental studies to attenuate cerebral ischemia and reperfusion injury.[45] However, because of the short half-life and inefficient crossing of the BBB

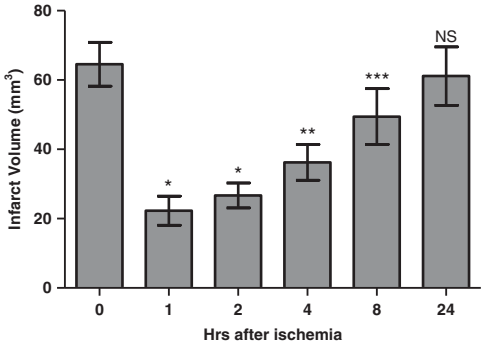

Figure 6. Therapeutic window of nanoparticles treatment. Mice were subjected to 1 hour of ischemia followed by 48 hours of reperfusion. Animals were administered PBCA/SOD nanoparticles at 1, 2, 4, 8, or 24 hours of reperfusion and then killed at 48 hours. Control, uninjected animals. Brains were subject to triphenyltetrazolium chloride (TTC) staining for infarct volumes. $N = 10$ per time point. $^{*}P < 0.01$; $^{**}P < 0.005$; $^{***}P < 0.001$; NS, not significant. PBCA, polybutylcyanoacrylate; SOD, superoxide dismutase.

makes it difficult for therapy. Conjugation of the SOD1 to polyethylene glycol increased the half-life in blood and showed a reduction in infarct volume.[45] Encapsulation of SOD1 in liposomes also increased the half-life, BBB penetration and uptake by neuronal also protected the brain from ischemic injury.[46,47] A recent study showed that nontargeted nanoparticle containment of SOD1 also protected the brain from ischemic injury and improved behavioral outcomes.[28] Reddy *et al*[28] have previously shown lack of therapeutic efficacy of free SOD administered intravenous, intracarotid, or intrajugular, in a rat ischemic stroke model similar to that used in the present study. The observed lack of efficacy was possibly because of the inability of the free enzyme to cross the BBB and its short half-life in the circulation (~6 minutes). Other studies have also shown lack of efficacy of exogenous SOD in ischemic stroke models.[16,48] Because prior literature data showed lack of the efficacy of the free enzyme, it has not been extensively studied in this work.

Retention of functionality on storage is a common concern for all enzyme- and protein-based drugs due to their poor stability. Conjugation to nanoparticulate carriers generally results in improved protein stability to unfolding, thermal treatment, or presence of denaturing agents.[49] We found that SOD-liposome conjugates showed remarkable storage stability in aqueous suspension, with ~60% of activity retained after incubation at 37°C for 120 days. Use of lyophilization in the presence of cryoprotectors allowed further improvement of storage stability. Results of accelerated aging study showed that lyophilized SOD liposomes retained ~80% of activity on storage at 37°C for 120 days, corresponding to the shelf-life of ~1 year at room temperature.

In vitro cell culture experiments showed that targeted SOD NPs were more efficient in protecting neurons from oxidative insult than the untargeted SOD NPs. One possible reason for this effect is that antibody-directed binding to NDMA R1 receptors improves cellular uptake of targeted NPs compared with the untargeted ones leading to higher intracellular drug concentration in the case of targeted NPs. These results are in good agreement with our previous cell culture studies, which showed preferential uptake of targeted anti-NR1-SOD NPs by rat cerebellar neurons.[31]

While preparing different delivery vehicles, it was not possible to achieve identical SOD and antibody loadings. For *in vivo* experiments, we chose to use fixed SOD dose (25 U per injection) and therefore had different concentrations of targeting antibody for different vehicles. Highest anti-NR1 antibody concentration *in vivo* was in the case of PBCA NPs; in the case of liposomes, its concentration was ~30% lower, and it was considerably (more than four times) lower in the case of bulk loaded PLGA NPs. Notably, in spite of these differences therapeutic effect was similar for different delivery vehicles coated by anti-NR1 antibody (Figure 4). A more detailed study of the effect of the SOD to targeting antibody ratio on therapeutic efficacy could help to determine whether it is possible to minimize antibody loading while maintaining the same therapeutic efficacy.

This study shows the ability of targeted nanoparticles to be effective in the reduction of infarct volume and improvement in behavior after cerebral ischemic injury. It confirms results of a previous study with nanoparticle delivered SOD but further shows the effectiveness of targeted nanoparticles and a reduction in apoptosis and inflammatory markers.[28] In addition, these studies show the effect of nanoparticle delivered SOD at various times after cerebral ischemia and reperfusion injury validating the clinical usefulness of the particles.

DISCLOSURE/CONFLICT OF INTEREST

The authors declare no conflict of interest.

REFERENCES

1 Borgens RB, Liu-Snyder P. Understanding secondary injury. *Q Rev Biol* 2012; **87**: 89–127.
2 Tuttolomondo A, Di Sciacca R, Di Raimondo D, Arnao V, Renda C, Pinto A *et al*. Neuron protection as a therapeutic target in acute ischemic stroke. *Curr Top Med Chem* 2009; **9**: 1317–1334.
3 Yang Y, Rosenberg GA. Blood-brain barrier breakdown in acute and chronic cerebrovascular disease. *Stroke* 2011; **42**: 3323–3328.
4 Chen H, Yoshioka H, Kim GS, Jung JE, Okami N, Sakata H *et al*. Oxidative stress in ischemic brain damage: mechanisms of cell death and potential molecular targets for neuroprotection. *Antioxid Redox Signal* 2011; **14**: 1505–1517.
5 Allen CL, Bayraktutan U. Oxidative stress and its role in the pathogenesis of ischaemic stroke. *Int J Stroke* 2009; **4**: 461–470.
6 Adibhatla RM, Hatcher JF. Phospholipase A(2), reactive oxygen species, and lipid peroxidation in CNS pathologies. *BMB Rep* 2008; **41**: 560–567.
7 Yu G, Hess DC, Borlongan CV. Combined cyclosporine-A and methylprednisolone treatment exerts partial and transient neuroprotection against ischemic stroke. *Brain Res* 2004; **1018**: 32–37.
8 Amador M, Guest J. An appraisal of ongoing experimental procedures in human spinal cord injury. *J Neurol Phys Ther* 2005; **29**: 70–86.
9 Chan PH. Reactive oxygen radicals in signaling and damage in the ischemic brain. *J Cereb Blood Flow Metab* 2001; **21**: 2–14.
10 Chan PH. Oxygen radicals in focal cerebral ischemia. *Brain Pathol* 1994; **4**: 59–65.
11 Kontos HA, George E. Brown Memorial Lecture: oxygen radicals in cerebral vascular injury. *Circ Res* 1985; **57**: 508–516.
12 Siesjö BK, Agardh CD, Bengtsson F. Free radicals and brain damage. *Cerebrovasc Brain Metab Rev* 1989; **1**: 165–211.
13 Francis JW, Ren J, Warren L, Brown Jr RH, Finklestein SP. Postischemic infusion of Cu/Zn superoxide dismutase or SOD:Tet451 reduces cerebral infarction following focal ischemia/reperfusion in rats. *Exp Neurol* 1997; **146**: 435–443.
14 Pong K. Oxidative stress in neurodegenerative diseases: therapeutic implications for superoxide dismutase mimetics. *Expert Opin Biol Ther* 2003; **3**: 127–139.
15 Saito A, Hayashi T, Okuno S, Nishi T, Chan PH. Modulation of the Omi/HtrA2 signaling pathway after transient focal cerebral ischemia in mouse brains that overexpress SOD1. *Brain Res Mol Brain Res* 2004; **127**: 89–95.
16 Warner DS, Sheng H, Batinic-Haberle I. Oxidants, antioxidants and the ischemic brain. *J Exp Biol* 2004; **207**: 3221–3231.
17 Liu TH, Beckman JS, Freeman BA, Hogan EL, Hsu CY. Polyethylene glycol-conjugated superoxide dismutase and catalase reduce ischemic brain injury. *Am J Physiol* 1989; **256**: H589–H593.
18 Matsumiya N, Koehler RC, Kirsch JR, Traystman RJ. Conjugated superoxide dismutase reduces extent of caudate injury after transient focal ischemia in cats. *Stroke* 1991; **22**: 1193–1200.
19 Armstead WM, Mirro R, Thelin OP, Shibata M, Zuckerman SL, Shanklin DR *et al*. Polyethylene glycol superoxide dismutase and catalase attenuate increased blood-brain barrier permeability after ischemia in piglets. *Stroke* 1992; **23**: 755–762.
20 Truelove D, Shuaib A, Ijaz S, Ishaqzay R, Kalra J. Neuronal protection with superoxide dismutase in repetitive forebrain ischemia in gerbils. *Free Radic Biol Med* 1994; **17**: 445–450.

21 Veronese FM, Caliceti P, Schiavon O, Sergi M. Polyethylene glycol-superoxide dismutase, a conjugate in search of exploitation. *Adv Drug Deliv Rev* 2002; **54**: 587–606.
22 Pun PB, Lu J, Moochhala S. Involvement of ROS in BBB dysfunction. *Free Radic Res* 2009; **43**: 348–364.
23 Spatz M. Past and recent BBB studies with particular emphasis on changes in ischemic brain edema: dedicated to the memory of Dr Igor Klatzo. *Acta Neurochir Suppl* 2010; **106**: 21–27.
24 Kuroiwa T, Ting P, Martinez H, Klatzo I. The biphasic opening of the blood-brain barrier to proteins following temporary middle cerebral artery occlusion. *Acta Neuropathol* 1985; **68**: 122–129.
25 Klatzo I. Brain oedema following brain ischaemia and the influence of therapy. *Br J Anaesth* 1985; **57**: 18–22.
26 Klatzo I. Blood-brain barrier and ischaemic brain oedema. *Z Kardiol* 1987; **76**: 67–69.
27 Reddy MK, Wu L, Kou W, Ghorpade A, Labhasetwar V. Superoxide dismutase-loaded PLGA nanoparticles protect cultured human neurons under oxidative stress. *Appl Biochem Biotech* 2008; **151**: 565–577.
28 Reddy MK, Labhasetwar V. Nanoparticle-mediated delivery of superoxide dismutase to the brain: an effective strategy to reduce ischemia-reperfusion injury. *FASEB J* 2009; **23**: 1384–1395.
29 Lin Y, Pan Y, Shi Y, Huang X, Jia N, Jiang JY. Delivery of large molecules via poly(butyl cyanoacrylate) nanoparticles into the injured rat brain. *Nanotechnology* 2012; **23**: 165101.
30 Begley DJ. Delivery of therapeutic agents to the central nervous system: the problems and the possibilities. *Pharmacol Therap* 2004; **104**: 29–45.
31 Reukov V, Maximov V, Vertegel A. Proteins conjugated to poly(butyl cyanoacrylate) nanoparticles as potential neuroprotective agents. *Biotech Bioeng* 2010; **108**: 243–252.
32 Hantel C, Lewrick F, Reincke M, Süss R, Beuschlein F. Liposomal doxorubicin-based treatment in a preclinical model of adrenocortical carcinoma. *J Endocrinol* 2012; **213**: 155–161.
33 Lopes de Menezes DE, Pilarski LM, Allen TM. In vitro and in vivo targeting of immunoliposomal doxorubicin to human B-cell lymphoma. *Cancer Res* 1998; **58**: 3320–3330.
34 Moussaieff A, Yu J, Zhu H, Gattoni-Celli S, Shohami E, Kindy MS. Protective effects of incensole acetate on cerebral ischemic injury. *Brain Res* 2012; **1443**: 89–97.
35 Yu J, Zhu H, Ko D, Kindy MS. Motoneuronotrophic factor analog GM6 reduces infarct volume and behavioral deficits following transient ischemia in the mouse. *Brain Res* 2008; **1238**: 143–153.
36 Mattson MP, Zhu H, Yu J, Kindy MS. Presenilin-1 mutation increases neuronal vulnerability to focal ischemia in vivo and to hypoxia and glucose deprivation in cell culture: involvement of perturbed calcium homeostasis. *J Neurosci* 2000; **20**: 1358–1364.
37 Ellsworth JL, Garcia R, Yu J, Kindy MS. Time window of fibroblast growth factor-18-mediated neuroprotection after occlusion of the middle cerebral artery in rats. *J Cereb Blood Flow Metab* 2004; **24**: 114–123.
38 Bromont C, Marie C, Bralet J. Increased lipid peroxidation in vulnerable brain regions after transient forebrain ischemia in rats. *Stroke* 1989; **20**: 918–924.
39 Lebel CP, Bondy SC. Sensitive and rapid quantitation of oxygen reactive species formation in rat synaptosomes. *Neurochem Int* 1990; **17**: 435–440.
40 Driver AS, Kodavanti PR, Mundy WR. Age-related changes in reactive oxygen species production in rat brain homogenates. *Neurotoxicol Teratol* 2000; **22**: 175–181.
41 Chan PH, Kinouchi H, Epstein CJ, Carlson E, Chen SF, Imaizumi S *et al.* Role of superoxide dismutase in ischemic brain injury: reduction of edema and infarction in transgenic mice following focal cerebral ischemia. *Prog Brain Res* 1993; **96**: 97–104.
42 Chan PH, Kawase M, Murakami K, Chen SF, Li Y, Calagui B *et al.* Overexpression of SOD1 in transgenic rats protects vulnerable neurons against ischemic damage after global cerebral ischemia and reperfusion. *J Neurosci* 1998; **18**: 8292–8299.
43 Kondo T, Reaume AG, Huang T-T, Carlson E, Murakami K, Chen SF *et al.* Reduction of CuZn-superoxide dismutase activity exacerbates neuronal cell injury and edema formation after transient focal cerebral ischemia. *J Neurosci* 1997; **17**: 4180–4189.
44 Kondo T, Reaume AG, Huang TT, Murakami K, Carlson E, Chen S *et al.* Edema formation exacerbates neurological and histological outcomes after focal cerebral ischemia in CuZn-superoxide dismutase gene knockout mutant mice. *Acta Neurochir* 1997; **70**(Suppl): 62–64.
45 He YY, Hsu CY, Ezrin AM, Miller MS. Polyethylene glycol-conjugated superoxide dismutase in focal cerebral ischemia–reperfusion. *Am J Physiol* 1993; **265**: H252–H256.
46 Chan PH, Longar S, Fishman RA. Protective effects of liposome-entrapped superoxide dismutase on posttraumatic brain edema. *Ann Neurol* 1987; **21**: 540–547.
47 Imaizumi S, Woolworth V, Fishman RA, Chan PH. Liposome-entrapped superoxide dismutase reduces cerebral infarction in cerebral ischemia in rats. *Stroke* 1990; **21**: 1312–1317.
48 Genovese T, Cuzzocrea S. Role of free radicals and poly(ADP-ribose)polymerase-1 in the development of spinal cord injury: new therapeutic targets. *Curr Med Chem* 2008; **15**: 477–487.
49 Lynch I, Dawson K. Protein-nanoparticle interactions. *Nanotoday* 2008; **3**: 40–47.

Supplementary Information accompanies the paper on the Journal of Cerebral Blood Flow & Metabolism website (http://www.nature.com/jcbfm)